Talanta 116 (2013) 1033–1039

Contents lists available at ScienceDirect

Talanta

journal homepage: www.elsevier.com/locate/talanta

Solid-phase supported profluorescent nitroxide probe for the determination of aerosol-borne reactive oxygen species

Mohamad Sleiman*, Hugo Destaillats, Lara A. Gundel

Indoor Environment Group, Environmental Energy Technologies Division, Lawrence Berkeley National Laboratory, 1 Cyclotron Road, MS 70-108B, Berkeley, CA 94720, USA

ARTICLE INFO

Article history:
Received 14 June 2013
Received in revised form
15 August 2013
Accepted 16 August 2013
Available online 23 August 2013

Keywords:
Free radicals
Proxyl fluorescamine
Dichlorofluorescin
Cigarette smoke
Ozone
NO_x

ABSTRACT

Reactive oxygen species (ROS) and free radicals play important roles in the chemical transformation and adverse health effects of environmental aerosols. This work presents a simple and sensitive method for sampling and analysis of ROS using a packed column coated with a profluorescent nitroxide scavenger, proxyl fluorescamine (PF). Quantification was performed by extraction and analysis using HPLC with fluorescence detection. For comparison, the conventional method of collecting aerosols into dichlorofluorescin (DCFH) aqueous solution was used as a reference.

The method was successfully applied to the determination of ROS in a model secondary organic aerosol (SOA) system generated by ozonolysis of nicotine, as well as in secondhand tobacco smoke (SHS). ROS concentrations between 50–565 nmol m^{-3} were detected in fresh SOA and SHS samples. After SHS aging for 22 h, 13–18% of the initial ROS mass remained, suggesting the presence of persistent ROS. The new method offers better stability and reproducibility along with sensitivity comparable to that of DCFH (method detection limit of 3.2 and 1.4 nmol m^{-3} of equivalent H_2O_2 for PF and DCFH respectively). The PF probe was stable during storage at room temperature and not reactive with ozone or NO_x, whereas DCFH in the particle-collecting liquid system was strongly influenced by ozone and NO_x interferences. This case study provides a good basis for employing solid-phase supported PF for field measurement of specific ROS in other combustion systems (i.e. biomass burning, candles, and diesel exhaust) and environmental aerosols.

1. Introduction

Air pollution is a well-recognized environmental problem and a serious public health concern that is estimated to be responsible for 3.1 million premature deaths worldwide every year and 3.2% of the global burden of disease [1]. While monitoring methods exist, air pollutants such as ozone, carbon monoxide (CO), nitrogen oxides (NO_x) and particulate matter (PM), measurement of the short-lived species commonly referred to as *reactive oxygen species* (ROS) remains a challenging problem because of their low concentrations and high reactivity. The term ROS is used to describe a variety of coexisting molecular species such as hydrogen peroxide (H_2O_2), hydroperoxides (ROOH) and radicals, e.g. hydroxyl ($HO^{\bullet}$), carbon centered ($C^{\bullet}$), peroxyl ($HOO^{\bullet}$, $ROO^{\bullet}$), and superoxide anion ($O_2^{-\bullet}$). ROS are generated in the gas phase and particles from ozonolysis and photochemical reactions in polluted air. ROS are also formed in motor vehicle emissions and through combustion of organic materials such as tobacco and wood [2–4]. Although endogenously produced ROS are essential to life (e.g. signal transduction, neurotransmission), exposure to "environmental" ROS is believed to induce excess ROS in living cells, thus causing oxidative stress that is implicated in various inflammatory effects, such as asthma, chronic bronchitis, ischemic heart disease and stroke, among others [5–7]. Besides the adverse health effects that ROS can cause, these species are drivers of numerous chemical processes in indoor and outdoor air, affecting the oxidative capacity of the atmosphere, aerosol formation and aging [8,9].

Prod. Type: FTPAs a consequence, there is a critical need for new and better methods to monitor these reactive molecules.

In recent years, a number of ROS sampling and monitoring methods have been developed [4,10–13]. The most common approaches involve (i) collection of particulate matter (PM) on filters for a long period of time (up to 24 h) followed by analysis of the filter extract with electron spin resonance (ESR) [13] or (ii) sampling aerosols into impingers containing fluorogenic probes (i.e. 2′,7′-dichlorodihydrofluorescin diacetate (DCFH-DA), dihydrorhodamine 6G, hydroxyphenylacetic acid) that react with ROS and either increase or decrease their fluorescence [9,14–17]. While ESR sensitivity is relatively low and requires a specialized and expensive spectrometer, fluorescence methodology offers high sensitivity

* Corresponding author. Tel.: +1 510 486 6402; fax: +1 510 486 7303.
E-mail address: msleiman@lbl.gov (M. Sleiman).

0039-9140/$ - see front matter © 2013 Elsevier B.V. All rights reserved.
http://dx.doi.org/10.1016/j.talanta.2013.08.024

and simplicity [18]. Several recent methods take advantage of the ability of some ROS to release the fluorescence of fluorophore-linked nitroxides [11,19,20]. These molecules trap carbon-centered radicals ($C^{\bullet}$) to yield stable alkoxyamines at close to diffusion-controlled rates (10^7–10^9 M^{-1} s^{-1}) [19,21,22] and are able to scavenge reactive oxygen species (ROS) such as peroxyl radicals ($ROO^{\bullet}$) [19,23,24]. Until present, these nitroxide probes have been successfully applied to detect $OH^{\bullet}$ and other ROS in gas and liquid media. The procedure typically involves reacting the nitroxide with methyl radicals ($CH_3^{\bullet}$) produced by the reaction of $OH^{\bullet}$ with dimethyl sulfoxide (DMSO) [11,25,26]. The aim of this study was to develop a new approach to trapping radical species (i.e. $C^{\bullet}$, $N^{\bullet}$ and $ROO^{\bullet}$) in aerosol systems by coating a nitroxide probe, proxyl-fluorescamine (PF) [27], on glass beads packed in stainless steel tubes. The fluorescent adducts are then analyzed by HPLC with fluorescence detection. The analytical performance of the new method was compared to the conventional sampling technique using DCFH in aqueous solution. The DCFH method is often used as a standard method for measuring a broad range of ROS in aerosol systems. Both sampling methods were applied to measure ROS in a model aerosol system generated by nicotine ozonolysis, as well as in secondhand cigarette smoke, a major source of ROS in indoor air [4]. Moreover, the aerosols generated for ROS measurement were characterized with real-time vacuum ultraviolet aerosol time of flight mass spectrometry (VUV–AMS) [28].

2. Experimental

2.1. Materials and chemicals

Fluorescent probes: Proxyl fluorescamine (PF), 5-(2-carboxyphenyl)-5-hydroxy-1-[(2,2,5,5-tetramethyl-1-oxypyrrolidin-3-yl)methyl]-3-phenyl-2-pyrrolin-4-on potassium salt, is a radical scavenger whose nitroxide moiety quenches the fluorescence of its nearby fluorophore group with its delocalized unpaired electron [29]. However, once PF traps a free radical (e.g. carbon-centered radicals), its fluorescence is restored by the conversion of the nitroxide to the corresponding spin-paired alkoxylamine (R′–N–OR) (Fig. 1-A) [30,31]. On the other hand, 2′,7′-dichlorodihydrofluorescin (DCFH) oxidizes to the fluorescent 2′,7′-dichlorofluorescin (DCF) in the presence of a broad range of ROS (Fig. 1-B). PF and DCFH: 2′,7′- dichlorodihydrofluorescin diacetate, were purchased from Invitrogen™ (Carlsbad, CA) and used without purification. H_2O_2 solution ($\geq$30%, TraceSELECT®) and Horseradish peroxidase type II were purchased from Sigma-Aldrich (St. Louis, MO). SKC® Midget Impingers (25 mL) were used for sampling with DCFH. The solvents (acetonitrile, water, and dimethyl sulfoxide) were of the highest purity available (HPLC grade). The glass beads used for trap loading had 3 mm diameter (Fisher Scientific), and were conditioned by washing sequentially with hexane, acetone and water then dried and stored in the dark at room temperature.

2.2. Generation of aerosols

2.2.1. Secondary organic aerosols (SOA)

The reaction of nicotine with ozone was used as a model system to generate SOA, as described previously [32]. Liquid nicotine F(5 μL, Sigma-Aldrich, purity 99%) was injected into each of two 40-L Tedlar bags (A and B), filled with 30-L dry air (RH∼0%). Two L of ozone was generated by UV irradiation (UVP Inc.) of pure air, and introduced into Bag B, corresponding to an initial concentration of 100 ppbv inside the bag (in the absence of reactive losses). The ozone concentration in the supply air was measured using a calibrated UV Photometric Ozone monitor, model API 400 (Advanced Pollution Instrumentation, Inc.). Ozone levels used in this study were realistic and comparable to those typically found in indoor environments in southern California and particularly when devices marketed as “air purifiers” are used to remove tobacco odors (100–300 ppbv) [33–34]. On the other hand, the initial concentration of nicotine inside the bag measured by ATD-GC–MS [28] was 810 μg m^{-3}. The use of such a high initial nicotine concentration was necessary for two reasons: (a) most of the nicotine partitioned to internal surfaces of the Tedlar bag

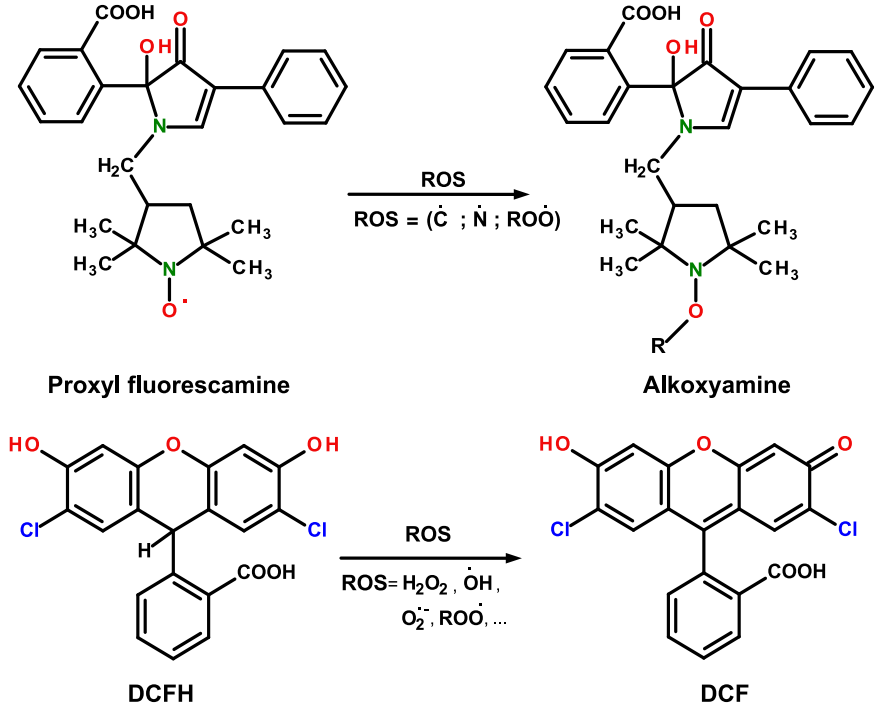

Fig. 1. Reactions of reactive oxygen species (ROS) with proxyl fluorescamine (PF) and dichlorofluorescin (DCFH). Upon oxidation with various ROS, DCFH is converted to 2′,7′-dichlorofluorescin (DCF), a fluorescent molecule. Proxyl fluorescamine is converted to a fluorescent alkoxyamine by reacting the nitroxide moiety with a carbon centered radical, a nitrogen centered radical or a peroxide (ROO).

during the reaction (30 min) and its concentration fell to 92 μg m^{-3}, and (b) the SOA yield from nicotine ozonolysis is relatively low (5–9%) and the sensitivity of the AMS requires a mass concentration of 20 μg m^{-3} or higher.

2.2.2. Secondhand cigarette smoke (SHS)

SHS was generated by smoldering one cigarette from a leading US brand in a 5-L glass vessel. During the first few minutes after smoking started the smoke was flushed into 100-L Tedlar bags filled with 70 L of zero air. The initial particle mass concentration in the bag was 890 μg m^{-3}. This concentration is comparable to the short-term peak concentrations found when smoking occurs in closed environments [35]. Note that SHS aging under the conditions of this study is not intended to mimic perfectly what happens in the real world, but to provide a controlled environment with minimum variables that allow for testing of our ROS methods and enable meaningful interpretation of the data.

2.3. Chemical characterization of aerosols

For aerosol chemical characterization, Tedlar bags containing secondhand smoke and SOA were characterized without further dilution using a scanning mobility particle sizer (SMPS, model 3936, TSI, Shoreview, MN) and an aerosol mass spectrometer (AMS) that vaporizes the aerosol on a heated deposition plate, followed by photoionization with tunable VUV, as detailed elsewhere [32].

2.4. ROS sampling methods

2.4.1. Preparation of solid-phase supported proxyl fluorescamine

5 g of conditioned and clean glass beads (35–40 mg weight; 3 mm diameter) were loaded into a 100-mL round bottom flask. A 10-mL aliquot of PF (100 mg L^{-1}) in water was added to the beads. The contents of the flask were mixed well manually and then dried by gentle heating at 40 °C in air. The coated beads were stored at –20 °C prior to use, for up to 2 days. For sampling, each stainless-steel trap (Perkin Elmer, 15 cm length and 0.6 cm diameter) was loaded with 30 coated beads (1.1–1.2 g) with an estimated PF loading of 250 μg per tube. The beads were held in place with a stainless steel mesh on the sampling inlet end and a small plug of quartz wool on the exit (See Supplementary material, Fig. S1). ROS sampling was carried out by drawing aerosol through two PF-coated traps, in series, at a flow rate of 0.1 L min^{-1} for a duration of 20 min (total volume of 2 L) using a peristaltic pump (Fig. 2). After sampling, each trap was flushed with 3 mL of acetonitrile and shaken gently for 5 min, before analysis using HPLC with UV/visible and fluorescence detection. Control blanks were generated by extracting a PF-coated trap in the same manner as a sample. For SOA, a Teflon filter was placed between the SOA bag and the inlet of the PF solid trap (and DCFH impinger), so that the contribution of the gas phase to ROS production could be measured. Some losses of gas phase species to the filter could occur in this approach and/or ROS could evaporate from the particles.

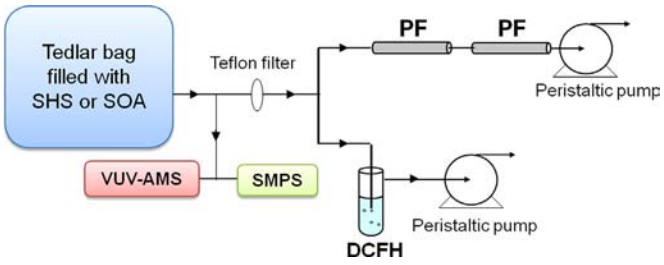

Fig. 2. Schematic of the experimental setup used for ROS sampling and characterization of secondhand smoke (SHS) and secondary organic aerosols (SOA). The Teflon filter was used only for SOA to separate the contribution of gases and particles to the ROS signal. A scanning mobility particle sizer (SMPS) and a vacuum ultraviolet aerosol mass spectrometer (VUV–AMS) were used for particle characterization.

2.4.2. Preparation of dichlorofluorescin (DCFH) impingers

DCFH was generated from its diacetate (H_2DCFDA) by alkaline hydrolysis: (a) 0.0049 g of H_2DCFDA was dissolved in 1 mL methanol, (b) 500 μL of this 10 mM H_2DCFDA solution was added to 2 mL of 0.01 N NaOH and kept in the dark at room temperature for 30 min, and (c) 10 mL of a 25 mM phosphate buffer at pH 7.4 was added to the H_2DCFDA/methanol/NaOH solution. Horseradish peroxidase (HRP) was added at 2.2 units HRP per mL to catalyze the reaction of DCFH with ROS during sampling. 300 μL of this solution was added to 15-mL aqueous solution in an impinger so that the final concentration of H_2DCFDA was 10 μM. The test aerosols were sampled simultaneously through the DCFH impinger and the PF traps (Fig. 2). For DCFH, sampling flow was set at 0.5 L min^{-1} for 20 min. The total sampling volume was limited to 10 L to allow collecting several ROS samples from the Tedlar bags filled with aerosols (60–100 L).

2.4.3. HPLC-fluorescence analysis of ROS samples

Collected ROS samples were analyzed by high performance liquid chromatography (HPLC, Agilent 1200 series) equipped with UV/visible and fluorescence detectors, on a C-18 column (4.6 × 150 mm). DCFH and its derivative (DCF) were eluted with a mobile phase 55/45 methanol/H_2O (modified with 20 mM Na_2PO_4 pH: 6.8) at flow rate of 0.7 mL min^{-1}. The fluorescence of DCF was measured with an excitation wavelength of 488 nm and an emission wavelength of 530 nm. PF was eluted with a 65/35 acetonitrile/water mobile phase at a flow rate of 0.7 mL min^{-1}. The PF fluorescence was measured with an excitation wavelength of 390 nm and an emission wavelength of 490 nm. Under these conditions, negligible interferences from naturally fluorescent smoke constituents occurred.

2.4.4. ROS calibration

As ROS include a variety of reactive compounds, it is difficult to establish a calibration curve for each chemical. Thus, calibration of the system was performed with standard H_2O_2 solutions with concentrations ranging from 0.1 to 1 μM, prepared by serial dilutions of a 30% stock solution of H_2O_2 [10]. The procedure for DCFH calibration followed in this study was similar to that of Hung et al. [10]. For calibration of PF we used the procedure developed by Blough et al. [20,22]: hydroxyl radicals were generated in solution through Fenton's reaction by mixing 0.1 mL of standard concentrations of H_2O_2 with 10 μM iron(II) sulfate heptahydrate $Fe(SO_4)\cdot 7H_2O$ and PF (10 mg L^{-1}) in a final volume of 3 mL of 5% DMSO in H_2O. The standard solutions and blanks were then incubated at room temperature for 30 min before HPLC analysis. The measured equivalent H_2O_2 concentration is an indicator of the reactivity of the ROS in a sample that had fluorescence intensity identical to that of an H_2O_2 solution of the calculated concentration:

$$X_{air} = 10^3 \times (C \times V_e)/V_s \quad (1)$$

$$X_{mg} = 10^3 \times (C \times V_e)/W \quad (2)$$

where X_{air} is the total concentration of ROS in the sample, expressed in nanomoles H_2O_2 m^{-3} of air; X_{mg} concentration of ROS in the particle phase, expressed in nanomoles H_2O_2 mg^{-1} of particles; C is the concentration of ROS in DCFH-HRP or in PF extracts, expressed in units of micromolar; V_e is volume of DCFH-HRP or PF solution,

expressed in liters; V_s is sample volume of sample, expressed in meter cube; W is the particle mass, determined by integrating the SMPS size distribution in the range 20–700 nm, expressed in milligrams, assuming a density of 1.1 g cm^{-3} for particles [36].

3. Results and discussion

3.1. Stability of ROS probes

The fluorescent probes must be stable for reliability in practical applications. Thus, the stabilities of DCFH and PF standards were examined. When stored at room temperature in the dark for 24 h, the DCFH working solution of 10 μM showed auto-oxidation, as shown by an increase of the fluorescence background signal by a factor of 3. To minimize this effect, stock solutions of DCFH were stored in the dark at −10 °C, and working solutions were prepared daily before sampling. On the other hand, glass beads coated with PF and stored in stainless-steel tubes at room temperature were found to be stable for at least 24 h without generation of any detectable artifact signal. This stability shows that PF solid traps can be practical for use in field measurements of ROS.

3.2. Linearity, precision, reproducibility and detection limits

As shown in Fig. 3, both methods were linear with H_2O_2 concentration over the range of 100–2000 nM, with acceptable correlation coefficients ($r^2 > 0.96$). Although DCFH was more sensitive than PF, the high y-intercept, corresponding to DCFH blank with no added H_2O_2, is a potential limitation for quantification of low levels of ROS. On the other hand, the y-intercept for the PF-trap was close to zero. This low background fluorescence shows minimal contamination of the beads by laboratory air and/or ambient light during coating of the glass beads and preparation of the PF-solid traps.

The instrumental precision of the HPLC analyses was determined from the reproducibility of four HPLC injections ($n=4$) of DCFH and PF standards under the same experimental conditions over a period of 2 days. The relative standard deviation (RSD) was 9.6% for DCFH and 6.2% for PF. The method reproducibility was determined by collecting SOA (from nicotine ozonolysis) using duplicate (side-by-side) of PF-solid traps and of DCFH impingers.

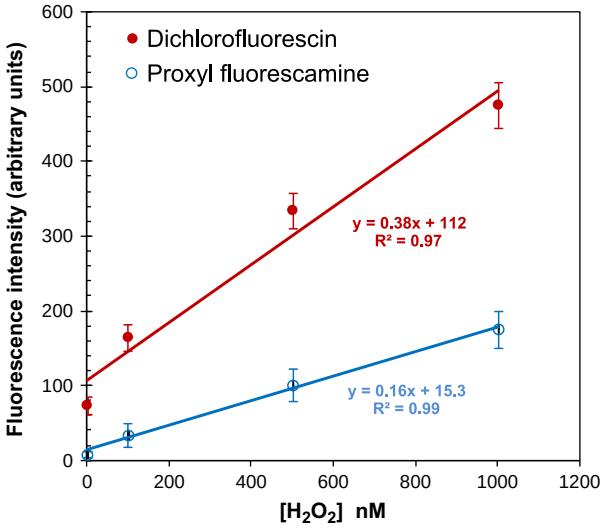

Fig. 3. Calibration curves for dichlorofluorescin (DCFH) and proxyl-fluorescamine (PF). DCFH calibration was performed using H_2O_2 solutions (0.1–1 μM) whereas PF calibration was based on generating hydroxyl radicals ($OH^{\bullet}$) through the Fenton reaction between H_2O_2 and iron(II) sulfate heptahydrate in DMSO/H2O (5:95 v-v).

The overall RSDs were 14% and 19% respectively, which is very reasonable given that this includes experimental errors due to preparation, sampling and analysis. Three method blanks were run by sampling a 60 L bag filled with zero air at 50% RH using the conditions described in Section 2.4. The method detection limit (MDL), defined as three times the standard deviation of method blanks, was estimated to be 1.4 and 3.2 nmol m^{-3} of equivalent H_2O_2 for DCFH and PF, respectively.

3.3. Measurement of ROS in secondary organic aerosols

Our previous work showed that nicotine, a major constituent of tobacco smoke, can be depleted substantially by its reaction with ambient ozone over timescales of minutes to hours. [32,37–39]. This reaction leads to the formation of stable gas phase products as well as SOA in the ultrafine range (< 100 nm) [32,38,40]. As shown in Fig. 4, after 30 min of nicotine-ozone reaction, a substantial level of particles was produced (46 μg m^{-3}) with a total number concentration of 6.5×10^4 particles cm^{-3} and a geometric median diameter of 98 nm. The particle number concentration was comparable to those found in indoor environments (10^3–10^4 particles cm^{-3}) [41–44]. The main constituents of the resulting SOA were include nicotine N-oxide (m/z 178), cotinine (m/z 176), nicotinamide (m/z 122), 3-acetaminopyridine (m/z 136), and dicarbonyl products (m/z 149, 190 and 206) such as 3-oxo-3-pyridin-2-ylpropanal (m/z 149). These products were found to be associated with high asthma hazard indices, indicating that they are likely to cause or exacerbate asthma [32]. The masses m/z 79 and 84 correspond to pyridine and pyrrolidine fragments of nicotine, respectively. Fig. 5 shows the concentrations of ROS produced in the SOA generated from nicotine ozonolysis, as well as the blank levels that account for the independent contributions of nicotine and ozone to the measured signal. The initial concentrations of nicotine and ozone in the separate blank samples and ROS sampling procedure were identical to those used for SOA samples (nicotine + ozone). As expected, very little ROS signal was measured for pure nicotine, suggesting that it does not interfere with the measurement of ROS using DCFH or PF (see Fig. 5). Ozone (100 ppbv) produced a significant background fluorescent signal when using DCFH, suggesting that measurements of ROS in ambient air using DCFH impingers may be influenced by ozone interference. In contrast, using a PF solid trap, very little signal was observed from ozone, indicating the suitability of PF for measuring ROS in indoor or ambient air samples where ozone is prevalent.

After ozone and nicotine reacted for 30 min, the total concentrations of ROS increased by a factor of 6–10 compared to blank levels. The ROS concentrations measured using PF range between

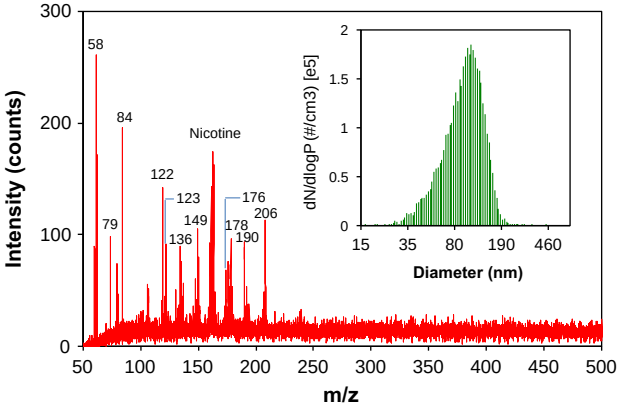

Fig. 4. Size distribution and mass spectrum of secondary organic aerosol formed after 30 min of reaction between nicotine and ozone (100 ppbv) in a 40-L Tedlar bag.

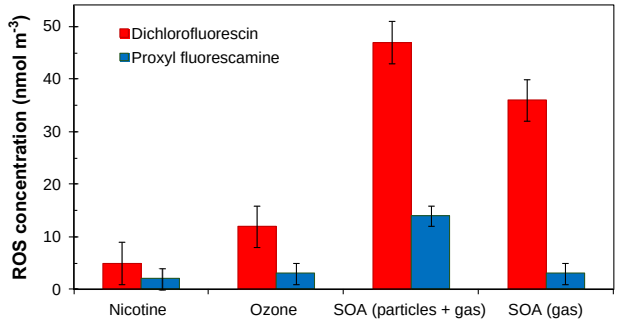

Fig. 5. ROS concentrations in secondary organic aerosols produced by nicotine reaction with ozone (100 ppbv) for 30 min in a 40-L tedlar bag. The contribution of the gas phase to ROS production was measured by placing a Teflon filter between the SOA bag and the inlets of the PF solid-trap and DCFH impinge. Method detection limits for DCFH and PF were 1.4 and 3.2 nmol m^{-3}, respectively.

4 nmol m^{-3} (gas phase) and 14 nmol m^{-3} (gas and particles). These levels are comparable to typical ROS levels measured in indoor (2–4 nmol m^{-3} [4]) and outdoor environments (6–12 nmol m^{-3}) [45], highlighting the potential of the PF-solid trap method for measuring ROS at realistic levels. On the other hand, ROS levels measured by the DCFH method were 36 nmol m^{-3} (gas phase) and 48 nmol m^{-3} (gas and particle). On a per SOA mass basis, the level of particle-bound ROS measured by DCFH was around 1 μmole mg^{-1} of equivalent H_2O_2. This concentration is about one order of magnitude higher than that previously reported [12] for SOA generated by ozonolysis of limonene (140–160 nmoles mg^{-1}). As consequence, SOA produced from the ozonolysis of nicotine should be considered as a potential strong source of ROS particularly in indoor environments where smoking occurs.

3.4. Measurement of ROS in aging secondhand tobacco smoke

Due to the dynamic nature of tobacco smoke, it is essential to investigate the temporal dependence of ROS during the time between emission of SHS and inhalation (minutes to hours) in the indoor environment. To evaluate the effect of aging on ROS levels, samples were collected at three aging periods (1 h, 4 h and 22 h) with PF and DCFH probes. Simultaneously, chemical composition and size distribution of smoke particles were monitored in real-time (See Fig. S2) in an attempt to examine a possible correlation between ROS levels and aerosol size and composition. Overall, the particle mass concentration decreased by more than half (380 μg m^{-3} at 4 h vs. 890 μg m^{-3} at 0.5 h) because of particle deposition on internal surfaces of the Tedlar bag, while the composition remained largely unchanged. In both cases, the most intense signals were assigned to nicotine at *m/z* 162 and its pyrroldine fragment (*m/z* 84). A list of the observed mass signals assigned to cigarette smoke constituents was previously reported [32].

Fig. 6 presents the time dependence of H_2O_2 equivalent concentrations for SHS during aging in the Tedlar bag. ROS concentrations in fresh SHS were 565 ± 53 and 85 ± 9 nmol m^{-3} as measured by DCFH and PF, respectively. When expressed in mass concentrations of SHS these levels corresponded to 634 ± 59 and 95 ± 10 nmol mg^{-1}, respectively. These levels were corrected by applying the particle collection efficiency for PF and DCFH. The efficiency for the PF-solid trap was higher than 80% as measured by using two PF traps in series and analyzing the backup PF-trap as well as monitoring the particle concentration downstream using the SMPS. On the other hand, the trapping efficiency of the DCFH impinger was 20 ± 5% as estimated by measuring particle breakthrough with SMPS. Table S1 compares the results from this study to previously reported concentrations of ROS in secondhand tobacco smoke. Despite differences in instrumentation, cigarette

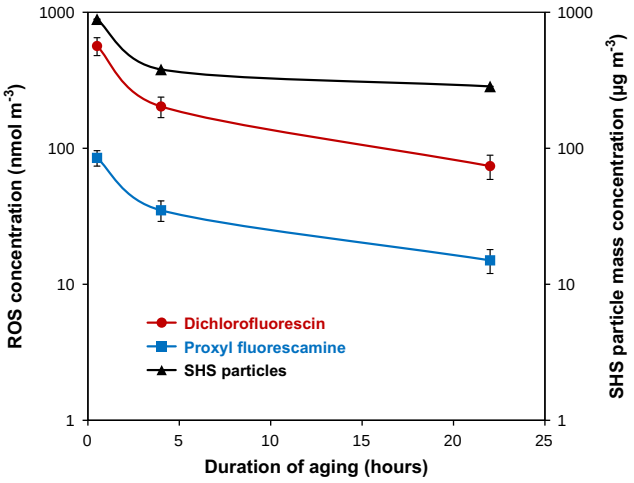

Fig. 6. Evolution of ROS concentrations and particle mass concentration during aging of secondhand smoke (SHS) in a 100-LTedlar bag. The initial particle mass concentration of SHS in the bag was 890 μg m^{-3}.

brands, and sampling protocols, the ROS levels measured in our study and previous ones are within the same order of magnitude.

The large difference in the ROS levels between DCFH and PF is likely due to the specificity of the PF probe which reacts only with a few types of free radicals (e.g. $C^{\bullet}$, $N^{\bullet}$, $ROO^{\bullet}$) whereas the DCFH is a non-specific probe of the oxidative capacity, including contributions of molecular species such as H_2O_2 and organic peroxides. While it is difficult from this study to infer the nature of the radicals detected, they may include peroxy radicals ($ROO^{\bullet}$), N-centered radicals ($N^{\bullet}$), semiquinone ($QH^{\bullet}$) [46], acyl ($R–C^{\bullet}=O$) and alkylaminocarbonyl radicals ($R–N–C^{\bullet}=O$) [47].

During aging, the ROS and SHS aerosol mass concentrations decreased significantly following similar trends, suggesting that a large fraction of the ROS detected was associated with SHS particles. After 22 h of aging, about 13–18% of the initial ROS mass remained. Given the very short lifetime of ROS (seconds to minutes), it is intriguing that a significant residual ROS remained even after 22 h of SHS aging. Several reasons can explain these results:

(i) Continuous formation of ROS within smoke plumes via dynamic processes involving reactions of species such as NO, NO_2, O_2, and incompletely oxidized organic compounds [48,49], as illustrated in Eq. (3)–(6):

$$R^{\bullet} + O_2 \rightarrow ROO^{\bullet} \quad (3)$$

$$ROO^{\bullet} + NO \rightarrow RO^{\bullet} + NO_2 \quad (4)$$

$$ROO^{\bullet} + NO_2 \leftrightarrow ROONO_2 \quad (5)$$

$$RO^{\bullet} + NO \rightarrow RONO \quad (6)$$

To test this hypothesis, NO_x and ROS were measured during the aging of SHS. Over 22 h of aging the NO_x levels remained stable (NO: 50–55 ppbv and NO_2: 0.5–1 ppbv) as measured with a chemiluminiscence detector (Teledyne APT 400). To find out if similar levels of NO_x could contribute to the ROS signal, we measured the fluorescence response of DCFH and PF by sampling a 20-L bag filled with 55 ppbv NO and 2 ppbv NO_2 in air. The fluorescence signal with PF probe was below the detection limit, whereas DCFH produced a small response with equivalent ROS concentration of 7 nmol m^{-3}. This level corresponded to about 8% of the ROS concentration measured for SHS aged for 22 h, indicating that NO and NO_2 interfere in DCFH measurements but cannot alone explain the ROS observed in aged SHS.

(ii) The existence of persistent free radicals that are stabilized on the surface of particles [50–53]. Recently, "environmentally persistent free radicals" (EPFRs) have been reported in post-combustion particles with lifetime ranging from days to weeks [53]. These EPFRs are possibly formed via reaction with transition metal oxides (e.g. CuO and ZnO) that can be easily reduced by a chemisorbed organic compound (e.g. hydroquinone, catechol, and phenol) converting the metal to a lower oxidation state. During this process, an organic surface-bound resonance-stabilized radical (e.g. semiquinone, phenoxyl, cyclopentadienyl) is formed [52, 53] (see Eq. (7)):

$$M^{+n}\ldots(O)R(OH) \rightarrow M^{+n-1}\ldots(O)R^{\bullet}(OH) \leftrightarrow M^{+n-1}\ldots(O^{\bullet})R(OH) \quad (7)$$

EPFRs associated with reduced metal oxides could interact synergistically to produce ROS (superoxide, hydrogen peroxide, and hydroxyl radicals) while regenerating the EPFR and the oxidized form of the transition metal. Because cigarette secondhand smoke contains a myriad of potentially toxic organic compounds and metals (copper, arsenic, cadmium, chromium, and nickel), it is possible that such a mechanism of formation of EPFRs occurs. However, the contribution of transition metals in SHS to the observed ROS and $R^{\bullet}$ activity was not addressed in this study. Therefore, the exact nature of EPFRs and their chemistries require additional studies to determine their origin and environmental impacts.

(iii) Re-suspension of ROS-bound particles from chamber walls after deposition. During aging, a significant fraction of particles deposit onto the internal surfaces of the Tedlar bag. However, these particles continue to carry stabilized radicals and could contribute to the formation of ROS. Thus, during ROS sampling, possible re-suspension of these particles can result in the detection of residual ROS in secondhand smoke.

4. Conclusions

This case study demonstrated a successful application of a simple and sensitive method for sampling and measuring ROS in aerosol samples (e.g. SOA and SHS) using solid phase trapping by proxyl fluorescamine and HPLC-fluorescence analysis. Because radicals are formed or persist during aging of smoke, they can be biologically important when smoke is inhaled, and can play an important role in the formation of hazardous chemicals in aged tobacco smoke, recently dubbed "thirdhand smoke" [28,40,54,55]. The PF-method offers significant advantages over the conventional DCFH-impinger method, including the simplicity of sampling onto solid supports, improved stability of the probe and radical adducts, and minimum interference from ozone and NO_x. Moreover, the better selectivity of proxyl fluorescamine can be used to determine the contribution of free radicals such as $C^{\bullet}$ $N^{\bullet}$, and $ROO^{\bullet}$ to particulate and gaseous oxidants in aerosols. This could allow exploring the health effects of specific radicals and identify correlations with sources, compared the type of method that is sensitive to many types of ROS. This new approach can be easily adapted to measure radicals emitted by other sources (biomass smoke, black carbon, diesel exhaust, etc.) using proxyl fluorescamine or other pro-fluorescent nitroxide probes.

Acknowledgments

This research was supported by the California Tobacco-Related Disease Research Program (TRDRP) Grant nos. 18FT-0105 and 20KT-0051. H.D. and L.G. were supported by TRDRP Grant no. 20PT-0184, subproject 6823sc. LBNL operates under US DOE Contract no. DE-AC02-05CH11231. The authors are grateful to Musahid Ahmed, Kevin Wilson, and Theodora Nah from the Chemical Dynamics group at the Advanced Light Source (ALS at LBNL), for their assistance with the analysis of SOA and cigarette smoke aerosol. We also thank Regine Goth-Goldstein and Bo Hang for their valuable suggestions.

Appendix A. Supplementary material

Supplementary data associated with this article can be found in the online version at http://dx.doi.org/10.1016/j.talanta.2013.08.024.

References

[1] WHO, ⟨http://www.who.int/ipcs/features/air_pollution.pdf⟩, 2009.
[2] H.F. Hung, C.S. Wang, J Chin Inst, Chem. Eng. 37 (2006) 491–499.
[3] B. Miljevic, M.F. Heringa, A. Keller, N.K. Meyer, J. Good, A. Lauber, P.F. Decarlo, K. E. Fairfull-Smith, T. Nussbaumer, H. Burtscher, A.S.H. Prevot, U. Baltensperger, S. E. Bottle, Z.D. Ristovski, Environ. Sci. Technol. 44 (2010) 6601–6607.
[4] S.W. See, Y.H. Wang, R. Balasubramanian, Environ. Res. 103 (2007) 317–324.
[5] P.H. Danielsen, P. Moller, K.A. Jensen, A.K. Sharma, H.k. Wallin, R. Bossi, H. Autrup, L. Molhave, J.L. Ravanat, J.J. Briede, T.M. de Kok, S. Loft, Chem. Res. Toxicol. 24 (2011) 168–184.
[6] K. Donaldson, V. Stone, A. Seaton, W. MacNee, Environ. Health Perspect. 109 (2001) 523–527.
[7] N. Li, C. Sioutas, A. Cho, D. Schmitz, C. Misra, J. Sempf, M.Y. Wang, T. Oberley, J. Froines, A. Nel, Environ. Health. Perspect. 111 (2003) 455–460.
[8] W. Rattanavaraha, E. Rosen, H.F. Zhang, Q.F. Li, K. Pantong, R.M. Kamens, Atmos. Environ. 45 (2011) 3848–3855.
[9] A.K. Cho, C. Sioutas, A.H. Miguel, Y. Kumagai, D.A. Schmitz, M. Singh, A. Eiguren-Fernandez, J.R. Froines, Environ. Res. 99 (2005) 40–47.
[10] H.F. Hung, C.S. Wang, J. Aerosol. Sci. 32 (2001) 1201–1211.
[11] B. Miljevic, K.E. Fairfull-Smith, S.E. Bottle, Z.D. Ristovski, Atmos. Environ. 44 (2010) 2224–2230.
[12] X. Chen, P.K. Hopke, Indoor Air 20 (2010) 320–328.
[13] S.L. Baum, I.G.M. Anderson, R.R. Baker, D.M. Murphy, C.C. Rowlands, Anal. Chim. Acta. 481 (2003) 1–13.
[14] S. Becker, L.A. Dailey, J.M. Soukup, S.C. Grambow, R.B. Devlin, Y.C.T. Huang, Environ. Health Perspect. 113 (2005) 1032–1038.
[15] M.F. Huang, W.L. Lin, Y.C. Ma, Indoor Air 15 (2005) 135–140.
[16] B.X. Ou, D.J. Huang, Anal. Chem. 78 (2006) 3097–3103.
[17] P. Venkatachari, P.K. Hopke, B.D. Grover, D.J. Eatough, J. Atmos. Chem. 50 (2005) 49–58.
[18] N. Soh, Anal. Bioanal. Chem. 386 (2006) 532–543.
[19] J.P. Blinco, K.E. Fairfull-Smith, B.J. Morrow, S.E. Bottle, Aust. J. Chem. 64 (2011) 373–389.
[20] M. Jia, Y. Tang, Y.F. Lam, S.A. Green, N.V. Blough, Anal. Chem. 81 (2009) 8033–8040.
[21] A.L.J. Beckwith, V.W. Bowry, G. Moad, J. Org. Chem. 53 (1988) 1632–1641.
[22] D.J. Kieber, N.V. Blough, Free Radical Res. Commun. 10 (1990) 109–117.
[23] C. Aliaga, J.M. Juarez-Ruiz, J.C. Scaiano, A. Aspee, Org. Lett. 10 (2008) 2147–2150.
[24] B.P. Soule, F. Hyodo, K.i. Matsumoto, N.L. Simone, J.A. Cook, M.C. Krishna, J.B. Mitchell, Free Radical Biol. Med. 42 (2007) 1632–1650.
[25] T. Maki, N. Soh, T. Fukaminato, H. Nakajima, K. Nakano, T. Imato, Anal. Chim. Acta. 639 (2009) 78–82.
[26] X.-F. Yang, X.-Q. Guo, Analyst 126 (2001) 1800–1804.
[27] S. Park, H. Nam, N. Chung, J.-D. Park, Y. Lim, Toxicol. in Vitro 20 (2006) 851–857.
[28] M. Sleiman, L.A. Gundel, J.F. Pankow, P. Jacob III, B.C. Singer, H. Destaillats, Proc. Natl. Acad. Sci. USA 107 (2010) 6576–6581.
[29] N.V. Blough, D.J. Simpson, J. Am. Chem. Soc. 110 (1988) 1915–1917.
[30] J.L. Gerlock, P.J. Zacmanidis, D.R. Bauer, D.J. Simpson, N.V. Blough, I.T. Salmeen, Free Radical Res. Commun. 10 (1990) 119–121.
[31] D.J. Kieber, N.V. Blough, Anal. Chem. 62 (1990) 2275–2283.
[32] M. Sleiman, H. Destaillats, J.D. Smith, C.-L. Liu, M. Ahmed, K.R. Wilson, L.A. Gundel, Atmos. Environ. 44 (2010) 4191–4198.
[33] C.J. Weschler, Indoor Air-Int. J. Indoor Air Qual. Climate 10 (2000) 269–288.
[34] M.F. Boeniger, Am. Ind. Hyg. Assoc. J. 56 (1995) 590–598.
[35] R. Kamens, C.-T. Lee, R. Wiener, D. Leith, Atm. Environ. Part A. Gen. Top. 25 (1991) 939–948.
[36] P.J. Lipowicz, J. Aerosol. Sci. 19 (1988) 587–589.
[37] H. Destaillats, B.C. Singer, S.K. Lee, L.A. Gundel, Environ. Sci. Technol. 40 (2006) 1799–1805.
[38] L.M. Petrick, A. Svidovsky, Y. Dubowski, Environ. Sci. Technol. 45 (2011) 328–333.
[39] L. Petrick, H. Destaillats, I. Zouev, S. Sabach, Y. Dubowski, Phys. Chem. Chem. Phys. 12 (2010) 10356–10364.
[40] G.E. Matt, P.J.E. Quintana, H. Destaillats, L.A. Gundel, M. Sleiman, B.C. Singer, P. Jacob Iii, N. Benowitz, J.P. Winickoff, V. Rehan, P. Talbot, S. Schick, J. Samet, Y. Wang, B. Hang, M. Martins-Green, J.F. Pankow, M.F. Hovell, Environ. Health. Perspect. 119 (2011) 1218–1226.

[41] S. Johannesson, P. Gustafson, P. Molnar, L. Barregard, G. Sallsten, J. Expos. Sci. Environ. Epidemiol. 17 (2007) 613–624.
[42] T. Hussein, T. Glytsos, J. Ondracek, P. Dohanyosova, V. Zdimal, K. Hameri, M. Lazaridis, J. Smolik, M. Kulmala, Atmos. Environ. 40 (2006) 4285–4307.
[43] L. Wallace, Aerosol Sci. Technol. 40 (2006) 348–360.
[44] L. Morawska, C.R. He, G. Johnson, H. Guo, E. Uhde, G. Ayoko, Environ. Sci. Technol. 43 (2009) 9103–9109.
[45] Y. Wang, P.K. Hopke, L. Sun, D.C. Chalupa, M.J. Utell, J. Toxicol. (2011) 2011.
[46] W.A. Pryor, Free Radical Biol. Med. 13 (1992) 659–676.
[47] J.B. Wooten, Mini-Rev. Org. Chem. 8 (2011) 412–426.
[48] R. Cueto, W.A. Pryor, Vib. Spectrosc. 7 (1994) 97–111.
[49] W.A. Pryor, M. Tamura, D.F. Church, J. Am. Chem. Soc. 106 (1984) 5073–5079.
[50] B. Dellinger, L. Khachatryan, S. Masko, S. Lomnicki, Mini-Rev. Org. Chem. 8 (2011) 427–433.
[51] M. Shiraiwa, Y. Sosedova, A. Rouvière, H. Yang, Y. Zhang, J.P.D. Abbatt, M. Ammann, U. Pöschl, Nat. Chem. 3 (2011) 291–295.
[52] A.L. dela Cruz, W. Gehling, S. Lomnicki, R. Cook, B. Dellinger, Environ. Sci. Technol. 45 (2011) 6356–6365.
[53] W. Gehling, B. Dellinger, Environ. Sci. Technol. 47 (15) (2013) 8172–8178.
[54] S. Schick, Tob. Control. 20 (2011) 1–3.
[55] J.P. Winickoff, J. Friebely, S.E. tanski, C. Sherrod, G.E. matt, M.F. Hovell, R. C. McMillen, Pediatrics 123 (2009) e74–e79.